

Fabrication and Properties of Core-Shell Structure P(LLA-CL) Nanofibers by Coaxial Electrospinning

Li Xiaoqiang,^{1,2,3} Su Yan,^{1,2,3} Chen Rui,^{3,4} He Chuanglong,³ Wang Hongsheng,³ Mo Xiumei^{1,2,3}

¹Key Laboratory of Science and Technology of Eco-Textile, Donghua University, Shanghai 201620, China

²State Key Laboratory for Modification of Chemical Fibers and Polymer Materials, Donghua University, Shanghai 201620, China

³Institute of Biology Science and Biotechnology, Donghua University, Shanghai 201620, China

⁴College of Textiles, Donghua University, Shanghai 201620, China

Received 27 October 2007; accepted 27 July 2008

DOI 10.1002/app.29056

Published online 30 October 2008 in Wiley InterScience (www.interscience.wiley.com).

ABSTRACT: In this article, core-shell structure nanofibers were fabricated by coaxial electrospinning with biodegradable copolymer Poly(L-Lactic-ε-Caprolactone) [P(LLA-CL) 50 : 50] as shell and bovine serum albumin (BSA) as core. Morphology and microstructure of the nanofibers were characterized by scanning electron microscopy and transmission electron microscopy. The mechanical properties were investigated by stress-strain tests. *In vitro* degradation rates of the nanofibrous membranes were determined by measuring

their weight loss when immersed in phosphate-buffered saline (pH 7.4) for a maximum of 14 days. Release behavior of BSA was measured by an ultraviolet-visible spectroscopy, and the results demonstrated that BSA could release from P(LLA-CL) nanofibers in a steady manner. © 2008 Wiley Periodicals, Inc. *J Appl Polym Sci* 111: 1564–1570, 2009

Key words: electrospinning; P(LLA-CL); core-shell structure; drug delivery

INTRODUCTION

Electrospinning is a technique that utilizes electric force alone to drive the spinning process and to produce polymer fibers from solutions or melts. Unlike conventional spinning techniques (e.g., solution- and melt-spinning), which are capable of producing fibers with diameters in the micrometer range, electrospinning is capable of producing fibers with diameters in the nanometer range. Electrospun polymer nanofibers possess many extraordinary properties including small diameters and the concomitant large specific surface areas, a high degree of structural perfection and the resultant superior mechanical properties. Additionally, the nonwoven fabrics (mats) made of electrospun polymer nanofibers offer

a unique capability to control the pore sizes among nanofibers. Unlike nanorods, nanotubes, and nanowires that are produced mostly by synthetic, bottom-up methods, electrospun nanofibers are produced through a top-down nano-manufacturing process, which results in continuous and low-cost nanofibers that are also relatively easy to align, assemble and process into applications. Many synthetic and/or natural polymers including, but not limited to, Polylactide,¹ Poly(ε-Caprolactone),^{2,3} Poly(Glycolic-acid) (PGA),⁴ Poly(L-Lactide-co-Caprolactone),⁵ proteins (e.g., collagen),⁶ and polysaccharides (e.g., Chitosan)⁶ have been electrospun into nanofibrous mats as innovative scaffolds for growing various kinds of cells.

Some researchers had investigated the drug delivery systems by mixing drug and polymer into the same solution to fabricate nanofibers. During the process of electrospinning, drug particles tend to locate on the surface of nanofibers, which made a significant burst release in the initial stage.⁷ However, if drug and polymer could integrate into homogeneous nanofibers at a molecular level, the releasing of drugs would be more stable.^{7,8} Coaxial electrospinning is a very simple technique to fabricate continuous composite nanofibers with core-shell structure.^{9,10} For example, Poly(L-lactic acid) and tetracycline hydrochloride (TCH) were employed as the shell and core materials respectively, by coaxial

Correspondence to: M. Xiumei (xmm@dhu.edu.cn).

Contract grant sponsor: Natural Science Foundation of Shanghai; contract grant number: 07ZR14001.

Contract grant sponsor: Donghua University (111 Project), Shanghai, China; contract grant number: B07024.

Contract grant sponsor: Key Laboratory of Science and Technology of Eco-Textile.

Contract grant sponsor: Open Foundation of State Key Laboratory for Modification of Chemical Fibers and Polymer Materials.

Journal of Applied Polymer Science, Vol. 111, 1564–1570 (2009)
© 2008 Wiley Periodicals, Inc.

electrospinning, and the results showed a sustained TCH release from these fiber mats for a long time.¹⁰

The aim of our study was to fabricate core-shell structure biodegradable polymer nanofibers by coaxial electrospinning, and investigate the degradation and drug releasing properties. We used a random copolymer poly(L-Lactic- ϵ -Caprolactone) [P(LLA-CL)] as the shell material and bovine serum albumin (BSA) as drug core. The core-shell structure nanofibers were fabricated by coaxial electrospinning with the BSA and P(LLA-CL) dissolved in distilled water and 2,2,2-trifluoroethanol (TFE), respectively. This novel drug delivery system was investigated by the methods of scanning electron microscopy (SEM), transmission electron microscopy (TEM), Fourier transform infrared spectroscopy (FTIR), mechanical measurement, *in vitro* degradation, and drug release.

MATERIALS AND METHODS

Materials

All of the reagents and solvents were used without further purification. The copolymer P(LLA-CL) (Mw = 378,839, Mw/Mn = 2.7324) in this work has the composition of 50 mol % L-lactide. TFE was obtained from Shanghai Darui Finechem Co., Ltd. BSA was purchased from Sigma-Aldrich.

Shell solution was prepared by dissolving P(LLA-CL) in TFE with sufficiently stirring at the room temperature. P(LLA-CL) solution concentration was chose as 0.06 g/mL. Core solution was prepared by dissolving a certain amount of BSA in distilled water to make the concentration of 0.10 g/mL.

Coaxial electrospinning

Figure 1 shows the basic experimental setup for the coaxial electrospinning. The spinneret apparatus consisted the inner needle (inner diameter: 0.51 mm, outer diameter: 0.8 mm) and the outer one (inner diameter: 1.6 mm) coaxially placed by each other as shown in Figure 1. Two syringe pumps were used to deliver core and shell solutions through inner and outer needles, respectively. In the present work, a high voltage DC power supply was used to generate a maximum 20 kV voltage, and an aluminum foil was used as receiving plate to collect nanofibers. The distance between the tip of needles and receiving plate was 12 cm. All the processes of electrospinning were operating at room temperature with the relative humidity of 60%. The flow rates of core solution were set at 0.10, and 0.20 mL/h, and the shell solution was 1.0 mL/h. The result nanofibrous mats had the thickness of around 0.10-0.20 mm, and the prepared nanofibrous mats were placed in vacuum over night to remove the residual solvent.

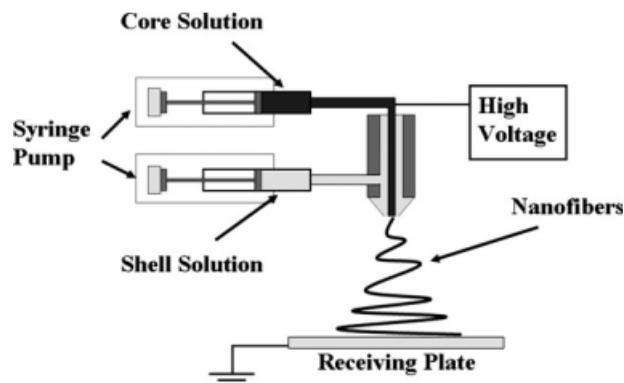


Figure 1 Experimental setup for the coaxial electrospinning process.

CHARACTERIZATION

Morphology of nanofibers was observed by digital vacuum scanning electron microscope (JSM-5600LV, Japan Electron Optical Laboratory) at the accelerating voltage of 15 kV. Samples for SEM observations were sputter coated with gold before observation. Verification of the core-shell structure was conducted by TEM (H-800, Hitachi) at 100 kV, and the samples for TEM observations were prepared by collecting the nanofibers onto carbon-coated Cu grids.¹⁰ The diameter of the electrospun ultrafine nanofibers was measured with image visualization software Image-J 1.34 (National Institutes of Health, Rockville, MD). Average fiber diameter and diameter distribution were determined by measuring about 100 random fibers from the SEM images.

FTIR study was carried out for detecting the presence of BSA in the nanofibers. The core-shell structure nanofibers mats collected on the aluminum foil were peeled up carefully, and then washed by distilled water for three times. The obtained nanofibrous mats cut into pieces, and BSA powder was compressed into films containing KBr pellets, respectively. The result pellets were tested by a FTIR spectrophotometer (Avatar 380, USA). All spectra were recorded by an absorption mode at 2 cm^{-1} intervals and in the wavelength range of $4000\text{-}400\text{ cm}^{-1}$.

Mechanical measurements were achieved by applying tensile test loads to specimens prepared from the coaxial electrospun nanofibers mats at the concentration and fluid flow rate mentioned previously. In this study, five specimens were prepared according to the method described by Huang et al.¹¹ First, a white paper was cut into templates with width \times length = 10×50 mm and double-side tapes were glued onto the top and bottom areas of one side. And then the aluminum foil was carefully peeled off and single side tapes were applied onto

the gripping areas as end-tabs. The resulting specimens had a planar dimension of width \times length = 10 \times 30 mm. Mechanical properties were tested by a materials testing machine (H5K-S, Hounsfield, England) at the temperature of 20°C and a relative humidity of 65% and a elongation speed of 10 mm/min. Three specimens were tensile tested to calculate the mean values and standard deviations for both pure P(LLA-CL) and BSA/P(LLA-CL) core-shell structure nanofibers mats.

***In vitro* degradation**

In this study, P(LLA-CL) nanofibrous mats were selected for the degradation measurements. The mats were cut into square pieces of 3.0 \times 3.0 cm, each one was weighted accurately as w_0 , and then was immersed into glass tube, which contained 10 mL of phosphate-buffered saline (PBS). The tubes were incubated in a 37°C water bath for the maximum up to 2 weeks. At the predetermined time points, triplicate mats samples were taken out of the tubes, washed with distilled water, and dried in vacuum at room temperature until it completely dried. The weight of sample after degradation recorded as w_i . The weight loss calculated as $\Delta w = w_0 - w_i$.

BSA release measurement

The core-shell structure nanofibers mats were cut into pieces with the weight of 0.28 ± 0.05 g. And then the nanofibers pieces were soaked in six tubes filled with 3.0 mL of PBS, respectively. The tubes with nanofibers mats were incubated at 37°C. At various time points, 1.5 mL of supernatant was retrieved from each tube and an equal volume of fresh PBS was replaced. The concentration of BSA in the supernatant was then determined by an ultraviolet-visible spectrophotometer (WFZ UV-2102 Unique Technology Shanghai) at an optical wavelength of 280 nm.

RESULTS AND DISCUSSION

Morphology of P(LLA-CL) nanofibers

P(LLA-CL) is easy to dissolve in many different solvents, such as acetone, chloroform, and 1,1,1,3,3,3-Hexafluoro-2-propanol. In this work, the water-miscible solvent TFE was used to prepare P(LLA-CL) solutions. Effect of polymer concentration in the range from 0.02 to 0.08 g/mL on fiber morphology was discussed. SEM micrographs of P(LLA-CL) nanofibers electrospun at different concentrations are shown in Figure 2. Different surface morphologies of the nanofibrous mats were observed with varied concentration of P(LLA-CL) solutions in TFE.

At the low concentrations of 0.02 and 0.04 g/mL, the electrospun nanofibers were stick together. With the increase of polymer concentration, the uniform fibers with less entanglement can be obtained. Fiber diameters were also affected by polymer concentration. The fiber diameter increased with the increasing of polymer concentration. This was coincident with the results mentioned by Mo et al.¹² It had also been found that the diameters distribution is not uniform. Some special thin fibers and some thick fibers occur in the SEM micrographs. It may be explained that the main fluid jet from the needle tip split into several subjects during the weeping process.¹³

Morphology of nanofibers fabricated by coaxial electrospinning

Morphology of core-shell nanofibers can be given by SEM micrographs as shown in Figure 3. Ultimate morphology of core-shell nanofibers with BSA cores was affected by core flow rate significantly. Experimental results have shown that when core solution flow rate was low as 0.10 mL/h, "bead-free" nanofibers were obtained. However, when the core rate was 0.20 mL/h, some bead-like nanofibers could be found [Fig. 3(b)]. This was likely due to the distilled water in the core solution being miscible with the TFE in the shell solution, resulting in a reduction of the P(LLA-CL) concentration, which would cause the bead generation. Furthermore, it was found that nanofibers generated from inner rate of 0.20 mL/h (average diameters, 380 ± 19 nm) were thinner than 0.10 mL/h (average diameters, 580 ± 24 nm). That because BSA was dissolved in PBS solution. With the increase of inner rate of coaxial electrospinning, there were more ions in nanofibers which made relative high conductivity compared with TFE and P(LLA-CL). Therefore, decrease of fiber diameters can be explained by conductivity increase of electrospinning solutions. This was similar to the previous results of Zong et al.¹

Figure 4 shows the TEM micrographs of core-shell structure of BSA/P(LLA-CL) nanofibers, which have a small fiber embed in a large fiber. The diameter of core fibers were ranging from 160 to 630 nm, and the shell fibers were 450-1540 nm.

FTIR study

The FTIR spectrum of BSA in Figure 5(a) depicts characteristic absorption bands at 1640, and 1540 cm^{-1} , which represent the amide I, II presented in proteins.⁶ Electrospun P(LLA-CL) has a characteristic peak of $-\text{COOC}-$ at 1735 cm^{-1} , and $-\text{CH}_2-$ at 1450 cm^{-1} as shown in Figure 5(b). The corresponding FTIR spectra was shown in Figure 5(c), which exhibited the characteristic peaks including BSA and

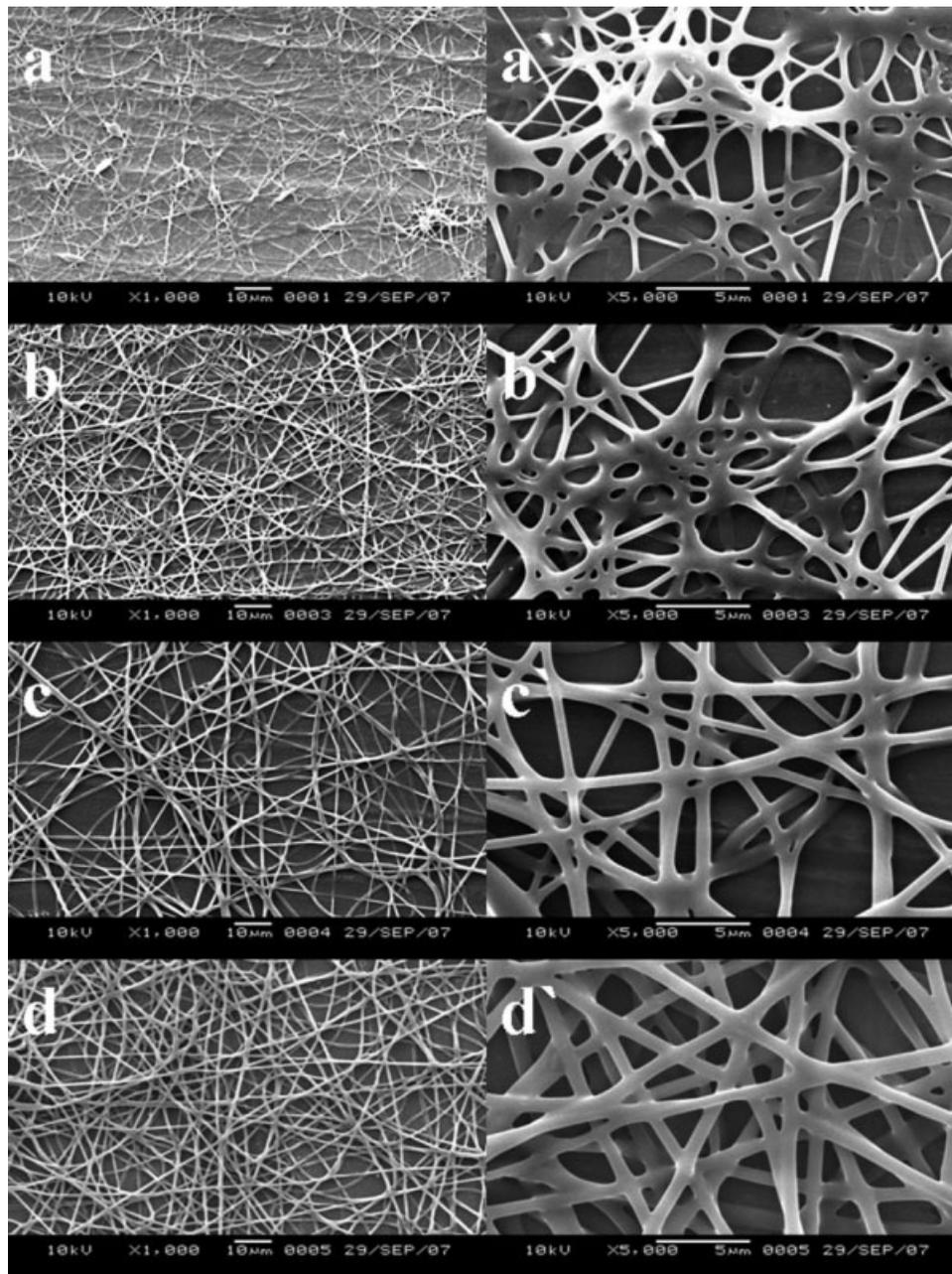


Figure 2 SEM images of P(LLA-CL) nanofibers mats electrospun from different concentration in TFE: (a) 0.02 g/mL P(LLA-CL) in TFE; (b) 0.04 g/mL; 0.06 g/mL and 0.08 g/mL. (a'-d') Show the high-magnification images of a-d, respectively.

P(LLA-CL). The results demonstrated that the material in core was BSA, because the core-shell structure nanofibers had been washed by distilled water and BSA on the surface of nanofibers could be dissolved in water completely. Furthermore, no new peak could be detected in Figure 5(c).

Mechanical behavior

Typical stress-strain curves of pure P(LLA-CL) and core-shell structure BSA/P(LLA-CL) nanofibrous mats were shown in Figure 6. BSA/P(LLA-CL)

nanofibrous mat showed the high module at the initial stage of the force given, and past a yield point with the stress of 0.5 MPa, thereafter, the stress increased with the increase of strain linearly. For P(LLA-CL) nanofibrous mat, there was a rubble-like stress-strain behavior. The average strength of P(LLA-CL) nanofibrous mat was 3.12 ± 0.18 MPa, and the average strain was $338 \pm 21\%$; for the core-shell nanofibers the number was 2.36 ± 0.13 MPa and $331 \pm 24\%$. This could be attributed to the "core-shell" structure of P(LLA-CL) nanofibers, for the BSA in core contributed much less mechanical

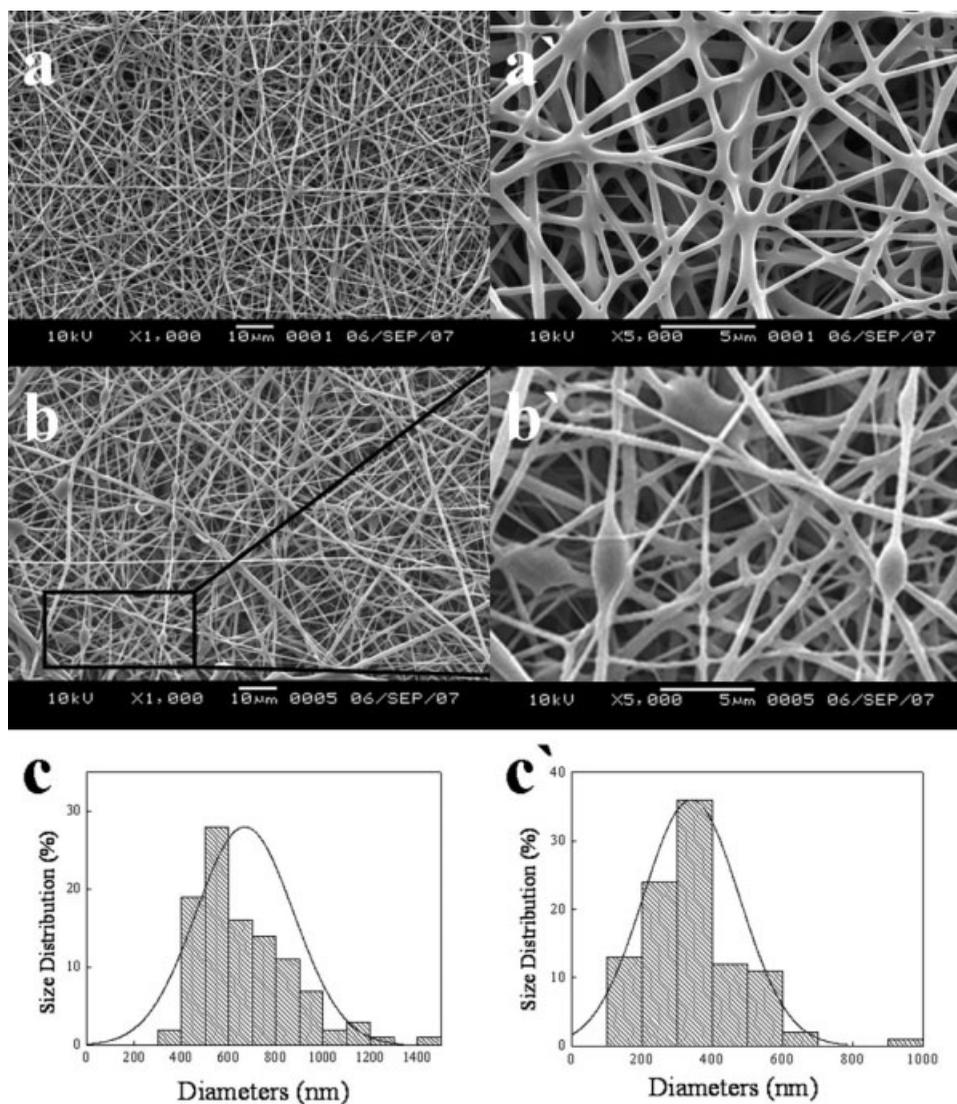


Figure 3 SEM micrographs of core-shell nanofibers of BSA/P(LLA-CL), (a) core solution flow rate was 0.10 mL/h; (b) 0.20 mL/h.

performance. It was noted that BSA could not be fabricated into nanofibers by electrospinning. A likely reason for this is that molecular weight of BSA is too low. This was coincident with the results

reported by other researchers.^{14,15} However, for drug delivery system, the key point was its ability of loading drugs or/and bioactive proteins. Relative low mechanical property of core-shell nanofibers has

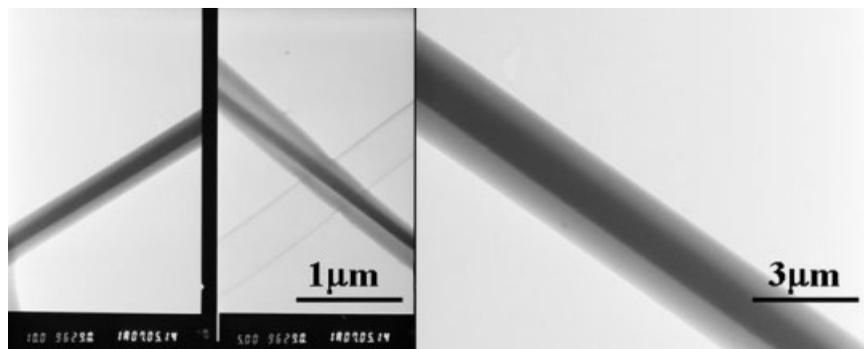


Figure 4 TEM micrographs of core-shell nanofibers.

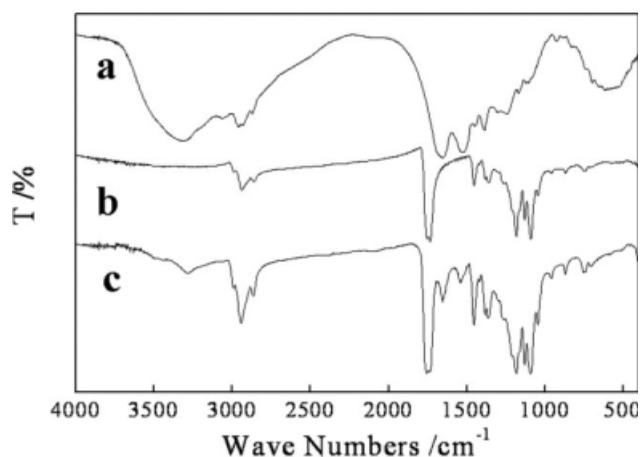


Figure 5 FTIR spectra of BSA, pure P(LLA-CL) nanofibers and their core-shell structure compound. (a) BSA, (b) pure P(LLA-CL) nanofibers, and (c) BSA/P(LLA-CL) core-shell structure compound.

no big influence to their application for the aim of drug delivery.

In vitro degradation

Although the main aim of this study was to investigate the property of electrospun P(LLA-CL) nanofibers as protein-encapsulated fibers, knowledge of the degradation of the polymer fibers helps in understanding of the protein release behavior. Furthermore, a biodegradable polymer-based scaffold must be able to support attachment and proliferation of cells, as well as maintaining suitable mechanical properties until tissue is regenerated at the injured site. An *in vitro* degradation study is carried out by measuring the weights of a sample before and after degradation in PBS. The weight losses of electrospun P(LLA-CL) nanofibers are shown in Figure 7. Sam-

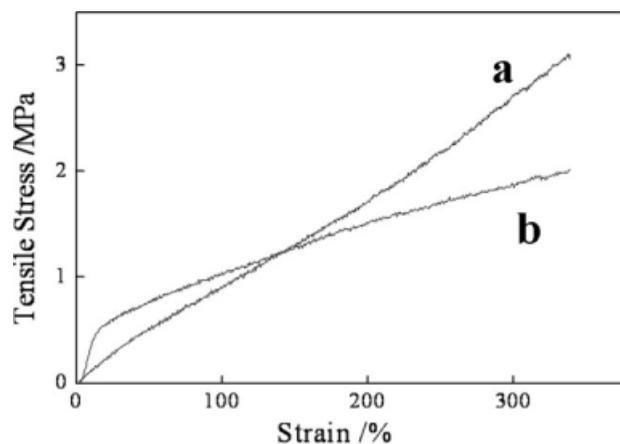


Figure 6 Mechanical property of nanofibers, (a) the stress-strain curves of pure P(LLA-CL) nanofibers; (b) the stress-strain curves of core-shell nanofibers of BSA/P(LLA-CL).

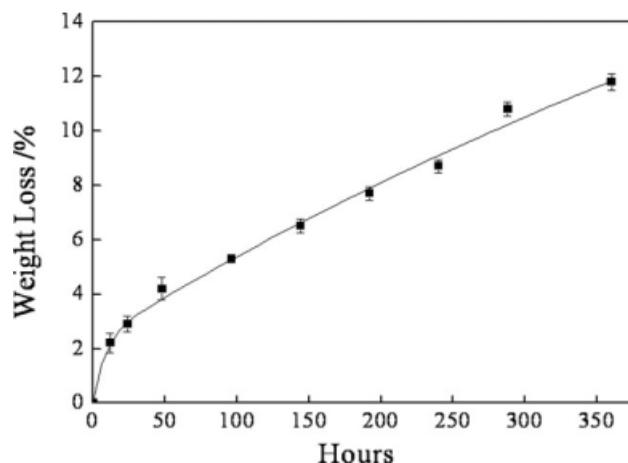


Figure 7 Mass loss of electrospun P(LLA-CL) nanofibrous mats incubated in PBS (pH 7.4) at 37°C.

ples used in these experiments were cut into 3.0×3.0 cm pieces and weights were about 35 ± 5 mg. Each time point gave the average of three samples and the error bars which indicated standard deviation. Significant mass loss was observed after tens of hours. The mass loss of the P(LLA-CL) nanofibers were gradually increased with increasing of incubation time. It reached to about 12% after incubating 14 days.

BSA release study

The BSA released description from electrospun nanofibers was shown in Figure 8. Sustained release of BSA from P(LLA-CL) nanofibers was obtained for up to 14 days. The release kinetics for the core-shell P(LLA-CL) nanofibers with BSA encapsulated can be illustrated in two stages: an initial burst of 25–30%, and then the protein was released in a relatively steady manner. The burst release behavior was

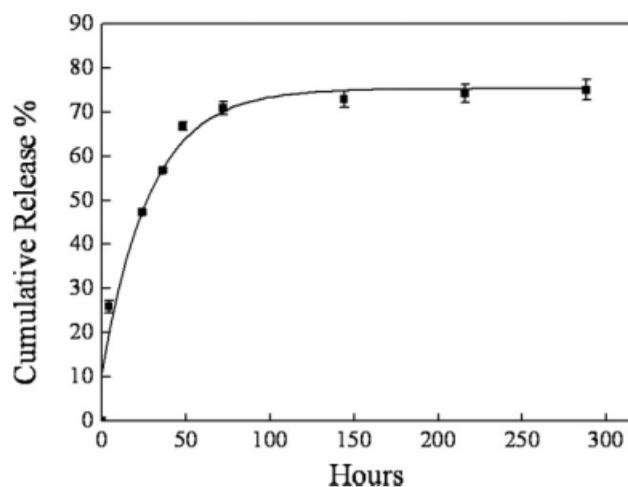


Figure 8 *In vitro* release of BSA from core-shell BSA/P(LLA-CL) nanofibers mats which incubated in PBS (pH 7.4).

probably caused by some of the BSA located on nanofibers surfaces.

In addition, we also introduced two hypotheses for the mechanism of BSA release. First, we hypothesized that diffusion was the predominant mechanism. The core-shell fibrous mesh system was modeled as a polydispersion of cylinders. And the transport mechanism was compared with an ideal case of a monodispersion of cylinders.

There were other mechanisms about drug release from nanofibers. The drug would undergo a two-release step, including an initial diffusion phase from the polymeric matrix and a second diffusion phase from aqueous pores formed in the polymer. Nanofibers mat which electrospun from a mixture of some drug and polymer, the drug is likely to conglomerate on the fibers surface. Therefore, a bad burst release of dissolved drug is generally observed in the initial stage. In the present core-shell structured composite nanofibers, the drugs were encapsulated inside the P(LLA-CL) carrier, which also can be released along with the biological degradation of nanofibers. Therefore, the drug release mainly relies on two different reasons, the polymer degradation and the diffusion of the drug through the fibers carrier.

CONCLUSIONS

Electrospinning is a simple and efficient method to make ultrafine and surface smooth fibers by polymer melts or solutions with diameters ranged from a few micrometers down to several nanometers. In this work, we have investigated core-shell structure nanofibers by coaxial electrospinning with BSA as core and P(LLA-CL) as shell. Micrographs of SEM and TEM demonstrated that nanofibers had smooth surface and the structure of core shell. For mechani-

cal properties, the average strength of P(LLA-CL) nanofibrous mat was 4.117 MPa, and the average strain was 338.4%; for the core-shell nanofibers the number was 2.356 MPa and 330.5%. *In vitro* degradation study showed that P(LLA-CL) nanofibrous mats loss about 12% weight after incubating in PBS(pH 7.4) at 37°C for 14 days. Release results demonstrated that BSA could release from P(LLA-CL) nanofibers in a steady manner.

References

1. Zong, X. H.; Kim, K.; Fang, D. F.; Ran, S. F.; Hsiao, B. S.; Chu, B. *Polymer* 2002, 43, 4403.
2. Yoshimoto, H.; Shin, Y. M.; Terai, H.; Vacanti, J. P. *Biomaterials* 2003, 24, 2077.
3. Zhang, Y. Z.; Wang, X.; Feng, Y.; Li, J.; Lim, C. T.; Ramakrishna, S. *Biomacromolecules* 2006, 7, 1049.
4. Sahoo, S.; Ouyang, H.; Goh, J. C. H.; Tay, T. E.; Toh, S. L. *Tissue Eng* 2006, 12, 91.
5. Zhu, Y.; Leong, M. F.; Ong, W. F.; Chan-Park, M. B.; Chian, K. S. *Biomaterials* 2007, 28, 861.
6. Chen, Z. G.; Mo, X. M.; Qing, F. L. *Mater Lett* 2007, 61, 3490.
7. Kenawy, E. R.; Bowlin, G. L.; Mansfield, K.; Layman, J.; Simpson, D. G.; Sanders, E. H.; Wnek, G. E. *J Control Release* 2002, 81, 57.
8. Zeng, J.; Yang, L. X.; Liang, Q. Z.; Zhang, X. F.; Guan, H. L.; Xu, X. L.; Chen, X. S.; Jing, X. B. *J Control Release* 2005, 105, 43.
9. Zhang, Y. Z.; Huang, Z. M.; Xu, X. J.; Lim, C. T.; Ramakrishna, S. *Chem Mater* 2004, 16, 3406.
10. He, C. L.; Huang, Z. M.; Han, X. J.; Liu, L.; Zhang, H. S.; Chen, L. S. *J Macromol Sci Phys B* 2006, 45, 515.
11. Huang, Z. M.; Zhang, Y. Z.; Ramakrishna, S.; Lim, C. T. *Polymer* 2004, 45, 5361.
12. Mo, X. M.; Weber, H. J. *Macromol Symp* 2004, 217, 413.
13. Deitzel, J. M.; Kleinmeyer, J.; Harris, D.; Tan, N. C. B. *Polymer* 2001, 42, 261.
14. Sun, B.; Duan, B.; Yuan, X. Y. *J Appl Polym Sci* 2006, 102, 39.
15. Huang, Z. M.; He, C. L.; Yang, A. Z.; Zhang, Y. Z.; Hang, X. J.; Yin, J. L.; Wu, Q. S. *J Biomed Mater Res A* 2006, 77, 169.